J Am Oil Chem Soc (2015) 92:439–447
DOI 10.1007/s11746-015-2594-7

ORIGINAL PAPER

Oleogels from Glycerol-Based Lyotropic Liquid Crystals: Phase Diagrams and Structural Characterization

Yael Cegla-Nemirovsky · Abraham Aserin · Nissim Garti

Received: 23 October 2014 / Revised: 18 December 2014 / Accepted: 6 January 2015 / Published online: 13 February 2015

Abstract In the course of our studies on structured reverse lyotropic liquid crystals (LLC) as oleogels, a system was designed with the desired physical and rheology properties for cosmetic and pharmaceutical applications. The aqueous phase was partially replaced by glycerol to minimize bacteriological problems and obtain specific rheology characteristics. The constructed phase diagrams are based on ternary mixtures of glycerol monooleate (GMO), decane, water, and glycerol. The main lyotropic mesophase obtained in this study was reverse hexagonal derived from dilution line 8:2 (72 wt% GMO and 18 wt% decane) and 10 wt% water; or water:glycerol (wt ratios 3:1 and 1:1) mixture. It was found that heat-cool fluctuation caused formation of new pseudo-equilibrium structures with mesomorphic transformations to more fluid and less ordered mesostructures. Replacing up to 50 wt% of the water by glycerol significantly increases the gel phase region in the phase diagram, meaning more structural compositional options. The structural parameters were determined using cross-polarized light microscopy (CPLM), differential scanning calorimeter (DSC), powder X-ray diffraction (PXRD), and small angle X-ray scattering (SAXS). Rheological measurements revealed viscoelastic properties of lyotropic liquid crystals with a decrease in the elasticity (G'), plasticity (G''), and complex viscosity (η^*), as a function of increasing the glycerol content.

Keywords Reverse hexagonal mesophases · Pseudo-ternary phase diagrams · SAXS · DSC · Rheology · Monoolein

Abbreviations

LLC	Lyotropic liquid crystal
GMO	Glycerol monooleate
CPLM	Cross-polarized light microscopy
DSC	Differential scanning calorimeter
PXRD	Powder X-ray diffraction
SAXS	Small angle X-ray scattering
LC	Liquid crystal
TAG	Triacylglycerol
DAG	Diacylglycerol
MAG	Monoacylglycerol
GMLi	Glycerol monolinoleate
SSL	Sodium stearoyl lactylate
Gly	Glycerol

Introduction

Oleogel is a dispersed system in oil continuous phase whose molecular interactions alter the physical properties of the oil, causing low fluidity and solid-like rheological properties. Its phase behavior depends on the type of oil that is gelled, presenting molecular interactions and at the same time crystallization and self-assembly [1]. Oleogels can be classified in two categories: polymeric organogels and low-molecular weight organogels. Low-molecular weight organogels are divided into two major classes: crystalline dispersions and lyotropic liquid crystalline (LLC) mesophases. The liquid

The results presented in this manuscript are part of Y. Cegla-Nemirovsky's dissertation as a partial fulfillment of the requirements towards a Ph.D. degree in Chemistry from the Hebrew University of Jerusalem, Israel.

Y. Cegla-Nemirovsky · A. Aserin · N. Garti (✉)
The Ratner Chair of Chemistry, Casali Center of Applied Chemistry, The Institute of Chemistry, The Hebrew University of Jerusalem, 9190401 Jerusalem, Israel
e-mail: garti@vms.huji.ac.il; garti@mail.huji.ac.il

crystals (LC) are a state of matter with intermediate properties between liquids and crystals. They have particular optical, electrical, and viscoelastic properties. The reverse LLC consist of cylinders or channels, made of nonionic surfactants and lipids, filled with hydrophilic liquids such as water or polyols [2, 3]. The crystalline dispersions are made of triacylglycerol (TAG) particles that trap the liquid TAG phase inside, forming a gel. The mechanical properties of the network depend on the size and shape of the crystals and the interactions between them [4, 5].

Oleogels can be made from diacylglycerols (DAG), monoacylglycerol (MAG) fatty acids [6, 7], wax esters, sorbitan monostearate, ceramides, [8, 9] and lecithin/sorbitan tristearate [10]. Some of the most important oleogel systems are those made with MAG. They have many different self-assembly structures, depending on the nature of the MAG, the amount of water, and the temperature. These structures are lamellar, micellar, cubic, and hexagonal mesophases [11, 12]. The most common reverse LLC are made of unsaturated monoglycerides of fatty acids such as: glycerol monooleate (GMO) or monolinoleate (GMLi). The main advantages of the LLC are their high water solubilization capacity and water-soluble guest molecules within their aqueous channels while maintaining a fat-like consistency [13, 14]. MAG can also form MAG–oil and MAG–oil–water systems that have only recently been studied [12, 15, 16]. In the oil system, below the gelation transition temperature, the inverse lamellar phase is formed with a definite hexagonal in-plane ordering and, below that point, a sub-α crystalline structure is seen [17, 18]. In MAG–oil–water systems there are hydrogen bond interactions that stabilize the structure and a lamellar gel is formed [19].

Oleogels have potential applications in food [20, 21], cosmetics [22], pharmaceuticals [23], and drug delivery [24]. For the food industry, Marangoni *et al*. [13] reported discovery of a new monoglyceride gel phase made from commercial HSK-A (10 % monopalmitin, 90 % monostearin), cosurfactants such as sodium stearoyl lactylate (SSL) or stearic acid, in a 20:1 (wt) ratio, Canola oil, and alkaline aqueous phase (0.05 N NaOH). This gel presented functionality similar to that of shortening or margarine and many unexpected health benefits, including an attenuated increase in serum triglyceride and insulin levels upon acute ingestion of this new phase relative to compositionally equivalent oil–water mixtures. Several cosmetic preparations such as lipsticks, lip balms, and creams have been suggested. Cosmetic organogels are also “delivery vehicles” as they deliver functional components such as moisturizers and coloring agents to the surface of the skin. Suzuki et al. [22] suggested formation of LC with branched alkyl surfactants and polyols composed of large amounts of oil (60 %) as a makeup remover. In addition, the formation of LC enhances the ability and functionality of cosmetics as carriers and they also add relative stiffness to the product in order to keep their shape inside their container [25, 26].

Amar-Yuli and Garti incorporated triacylglycerides (TAG) in the glycerol monooleate (GMO) to stabilize reverse hexagonal (H_{II}) mesophases at room temperature [27]. Amar-Yuli et al. [28] also showed that 72 wt% GMO, 8 wt% decane (9:1 wt ratio), 12 wt% water, and 8 wt% glycerol form an H_{II} structure that can facilitate the solubilization of proteins, such as insulin. In this study we used GMO as the surfactant [29], extensively studied as an essential component in the formation of cosmetic and drug delivery vehicles [28, 30, 31] along with decane as a nonpolar solvent, and glycerol as a water replacer in the inner phase of the LLC [28, 32].

Polyols are known to have strong effects on liquid crystals [33, 34]. Alam et al. [35, 36] demonstrated that the addition of glycerol to the water/$C_{12}EO_8$/dodecane system produced transitions from the cubic phase (I_1) and hexagonal phase (H_I) to H_I and lamellar (L_α) phases, respectively, at 25 °C and also caused a decrease in viscosity due to the microstructural transition. Additional studies are needed to explore the physical characteristics of type II (water-in-oil) LLC in the presence of polyols.

We structured an entire set of phase diagrams including 1:0, 3:1, and 1:1 wt% ratios of water:glycerol and characterized the structural composition, rheological properties and phase behavior of some samples. The effect of the variations in composition and temperature on the systems and its characteristics were also studied in order to obtain optimization and equilibrium of the structures.

Experimental

Materials

Distilled glycerol monooleate (monoolein, GMO) consisting of 97.1 wt% monoglycerides (fatty acid composition: 2.1 % myristic acid, 5.1 % palmitic acid, 4.4 % palmitoleic acid, 1.2 % stearic acid, 85.7 % oleic acid, 1.5 % linoleic acid), 2.5 wt% diglycerides, and 0.4 wt% free glycerol (acid value 1.2, iodine value 68.0, melting point 37.5 °C) was purchased from Riken Vitamin Co. (Tokyo, Japan). Decane (> 99 %) and glycerol (Gly) were purchased from Sigma Chemical Co. (St. Louis, MO, USA). The water was double distilled. All chemicals were used without further purification.

Sample Preparation

Three-component systems were prepared in two stages. First, GMO and decane in various weight ratios were mixed

and heated to 80 °C for homogenization. In the second stage, several determined weight ratios of water or water/glycerol were added to the mixtures at 80 °C and vortexed. After 10 min, immediately cooled to 25 °C, and allowed to rest a minimum of 24 h before examination. After cooling, the samples were incubated in water baths at 25 °C for 90 days and analyzed. After 90 days, the samples were heated to 37 °C for 60 additional days and the phase diagram composition was re-tested. After this stage the samples were finally cooled to 25 °C for 15 days with another phase diagram examination.

Visual Observations

Samples were determined to be "liquid isotropic", "turbid gel" and "soft gel" depending on their appearance and microscopical properties. They were analyzed at room temperature.

Cross-Polarized Light Microscopy (CPLM)

Samples were inserted between two glass microscope slides and observed with a Nikon light microscope Eclipse 80i model (Tokyo, Japan) equipped with cross-polarizers and attached to a digital Nikon DXM 1200C camera and a PC monitor.

Powder X-Ray Diffraction (PXRD)

Scattering measurements were performed on a Philips PW 1710 diffractometer with parallel-beam optics (Almelo, The Netherlands), 2° Soller slits for incident and diffracted beams, and 0.2 mm receiving slits. Monochromated Cu-Kα radiation was used. Samples were mounted on low-background quartz sample holders. XRD patterns were recorded in 10°–45° 2θ scale range at room temperature, 40 kV tube voltage, 30 mA tube current, and step scan mode with a scanning rate of 0.02° 2θ $(s)^{-1}$.

Small-Angle X-Ray Scattering (SAXS)

Scattering experiments were performed using a Be-filtered Cu Kα radiation (0.154 nm) from a rotating anode X-ray generator that operated at a power rating of 1.2 kW. The rotating anode diameter was 99 mm and its rotation speed was 9,000 rpm. The electron gun was a W filament. The X-ray radiation was further monochromated and collimated by Confocal Max-Flux Optics from Rigaku Inc. (Tokyo, Japan) and measured by a Mar345 Image Plate Detector from Marresearch (Norderstedt, Germany). The samples were held in 1.5 mm quartz X-ray capillaries inserted into an aluminum block sample holder. The camera constants were calibrated using silver behenate. The scattering patterns were implemented in the FIT2D software.

Differential Scanning Calorimetry (DSC)

The DSC measurements were carried out on a Mettler Toledo DSC822 (Greifensee, Switzerland) calorimeter, as follows: 10–15 mg of LLC samples were weighed using a Mettler M3 microbalance in standard 40 μL aluminum pans and immediately sealed by a mechanical press. The samples were cooled, using a liquid nitrogen cooling system, from 25 to −40 °C, at a rate of −5 °C min^{-1}, remained there for 5 min, and eventually were heated at 2 °C min^{-1} to 80 °C. An empty pan was used as a reference. The instrument determined the fusion temperatures of the solid components and the total heat transferred in any of the observed thermal processes. The enthalpy change associated with each thermal transition was obtained by integrating the area of the relevant DSC peak.

Rheology Measurements

Rheological measurements were performed using a Rheoscope 1 rheometer (Thermo-Haake, Karlsruhe, Germany). A cone-plate sensor was used with a diameter of 35 mm, cone angle of 1°, and a gap of 0.024 mm. The linear viscoelastic range (LVR) of a sample was determined before carrying out the oscillatory measurements. The storage and loss moduli were plotted as a function of stress at 1 Hz and 25 ± 0.2 °C. The shear moduli were independent of stress up to a critical applied stress and generally were observed to fall off sharply beyond the values of 100–120 Pa. These results indicate that the samples possess linear viscoelastic properties up to about 100–120 Pa. Above these typical values, the microstructure of the LLC phases breaks down, as reflected by the rapid decrease of the moduli. According to the determined LVR, the viscoelasticity measurements of dilution line 8:2 samples were generally performed at 75 Pa. Frequency-dependent rheological measurements were conducted in the range of 0–10 Hz. The viscoelasticity of the LLC phases was characterized in terms of the elastic modulus (G'), the loss modulus (G''), the complex viscosity (η^*), and the longest relaxation time (τ_{max}), according to the Maxwell model.

Results and Discussion

Composition and Structural Characterization

Phase Diagrams of Ternary Mixtures

The ternary phase diagrams of GMO, water, and decane are presented in Fig. 1. Observations revealed (Fig. 1a) the existence of two major self-assembled regions depicted as "fluid transparent isotropic phases" and, "soft transparent

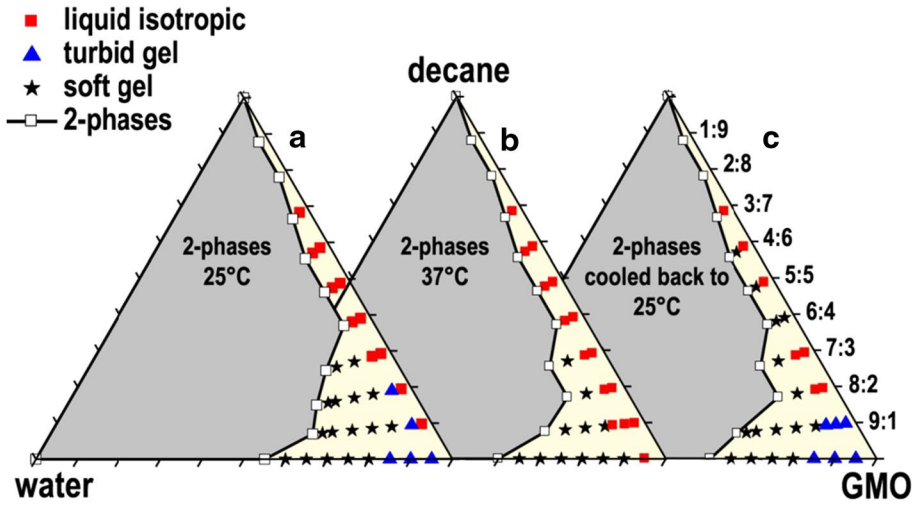

Fig. 1 Phase diagrams of GMO/decane/water (system I) at 25 °C (**a**) (90 days), 37 °C (**b**) (60 days), and recooling at 25 °C (**c**) (15 days)

Table 1 The effect of glycerol in GMO/decane/water:glycerol system at different temperatures

	L_1 area (%)	Soft gel area (%)	Turbid gel area (%)
I. GMO-decane-water at 25 °C	9.0	11.7	2.4
Heated to 37 °C	11.9	7.9	–
Cooled to 25 °C	5.6	11.9	4.2
II. GMO-decane-water: glycerol (wt ratio 3:1) at 25 °C	8.9	8.5	10.7
Heated to 37 °C	14.4	7.9	–
Cooled to 25 °C	5.0	15.8	1.7
III. GMO-decane-water: glycerol (wt ratio 1:1) at 25 °C	11.5	8.4	11.8
Heated to 37 °C	12.2	9.1	5.0
Cooled to 25 °C	9.1	8.7	9.6

L_1: liquid isotropic area

and turbid gels". Along the dilution with water (dilution lines 7:3, 8:2, and 9:1), there is a narrow isotropic liquid region at 25 °C, and a significantly wide gel phase [9 *vs* 14.1 % (11.7 + 2.4 % respectively see Table 1)]. After 90 days of storage at 25 °C, samples were reexamined, heated, to 37 °C and further aged (Fig. 1b) for 60 days. The elevated temperature enabled mobility of some components followed by slow and gradual rearrangement depicted as enlargement of the liquid isotropic region in the phase diagram and shrinkage of the gel phase (11.9 *vs* 7.9 %, respectively; see Table 1). Once the samples were cooled back to 25 °C (Fig. 1c) the liquid isotropic area shrank on the account of the gel phase [5.6 *vs* 16.1 % (11.9 + 4.2 % respectively see Table 1)], reaching a new equilibrium different from the one that we obtained initially (compare Fig. 1a and c). Formation of a new equilibrium took place due to the re-assembling of the components of the mesophases, after increasing the temperature (from 25 to 37 °C).

It is therefore clear that the mesophases under any given conditions are temperature-dependent and are not at real equilibrium, but are very dependent on the mobility of the components [37].

Phase Diagrams of Mixtures with Glycerol

Phase diagrams of systems in which part of the water (25 wt%) was replaced by glycerol (wt% ratio of 3:1) are shown in Fig. 2. The isotropic liquid region remains narrow and not much different from the one in which water was the aqueous phase (8.9 *vs* 9 %); see Table 1 and Fig. 2a. The main noticeable difference is in dilution line 6:4 of GMO:decane, the presence of glycerol exhibits a larger isotropic region, meaning less structured mesophases in which the nanometric droplets are completely disordered. On the other hand, in the presence of glycerol and along dilutions lines 7:3, 8:2 and 9:1 (richer in GMO) the gel phase region was larger, [total gel region 19.2 % (8.5 + 10.7 % respectively see Table 1) *vs* 14.1 % (11.7 + 2.4 % respectively see Table 1)]. However, the gel turned turbid, meaning a strong disorder of the lyotropic mesophase.

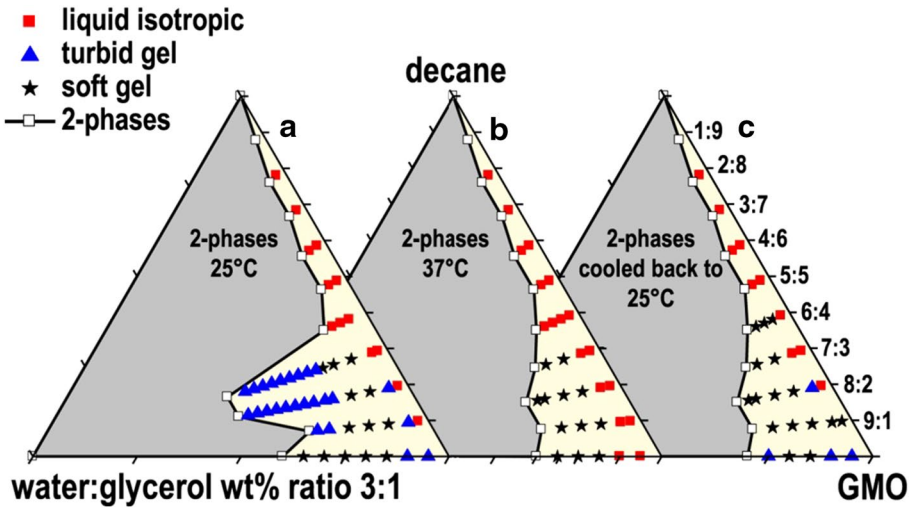

Fig. 2 Phase diagrams of GMO/decane/water:glycerol (wt% ratio 3:1) (system II) at 25 °C (**a**) (90 days), 37 °C (**b**) (60 days), and re cooling at 25 °C (**c**) (15 days)

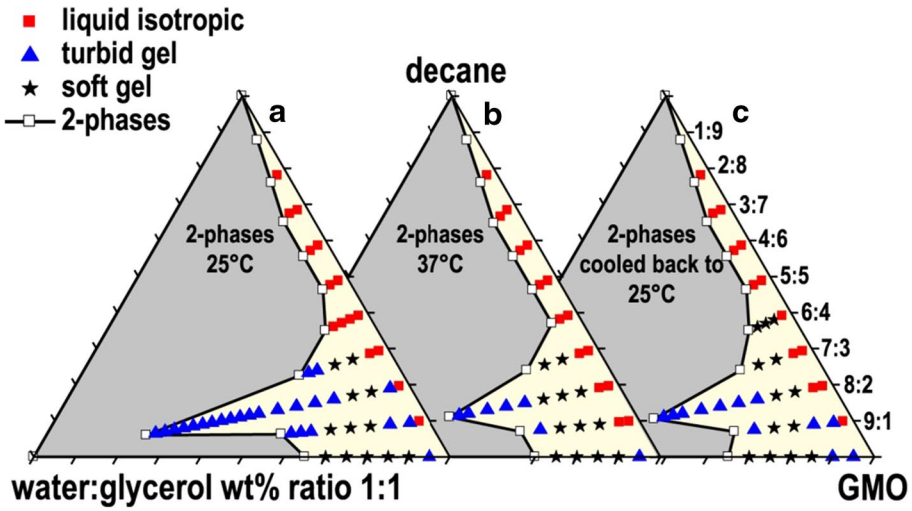

Fig. 3 Phase diagrams of GMO/decane/water:glycerol (wt% ratio 1:1) (system III) at 25 °C (**a**) (90 days), 37 °C (**b**) (60 days), and recooling at 25 °C (**c**) (15 days)

When 50 wt% water was replaced by glycerol (wt% ratio 1:1) (Fig. 3) the structural transformation was more pronounced. Larger isotropic regions at lower GMO content were recorded compared to the GMO/decane/water diagram (Fig. 1a), and the gel region significantly increased [19.2 (8.4 + 11.8 % respectively see Table 1) *vs* 14.1 (11.7 + 2.4 % respectively see Table 1)]. The major changes took place mainly at GMO-rich dilution lines (8:2, 9:1) but less in line 7:3. The heating–cooling (Fig. 3b, c) cycle confirms mainly shrinkage of the total gel phase.

The Effect of Glycerol

At 25 °C, the presence of glycerol in the system results in a small enlargement of the liquid isotropic area, shrinkage of the soft gel area, and enlargement in the turbid gel area (Table 1). This means that glycerol, being a chaotropic agent [35, 36], disorders the mesophases and forms liquid isotropic (L_1) with chaotically dispersed droplets instead of the LLC mesophases.

Increasing the temperature from 25 to 37 °C led to an increase in the L_1 area, and a decrease in the soft gel (system I and II) and the turbid area. When recooling the mesophase to 25 °C, the liquid region shrunk but the total region of the gel phase remained unchanged (Figs. 1, 2, and 3c), reaching a new equilibrium as a result of lowering the mobility of the system. Since the structural differences between the soft gel and the turbid gel are not clear, it was essential to conduct a more detailed structural study using advanced analytical tools. From a previous study [38], we learned that under certain conditions the turbid gels might have been of "small crystals of the GMO" (alone or in admixture) that could have been crystallizing out from the mixture. The PXRD measurements were very instrumental in clarifying this assumption.

PXRD Analysis

PXRD analysis showed that in all the compositions, in a dilution line 8:2 of GMO:decane (72 % GMO, 18 % decane, and 10 wt% water; or wt% ratio 3:1 and 1:1 water:glycerol) there is no crystalline matter (data not shown), meaning that the turbid mesophases are solely of oleogel.

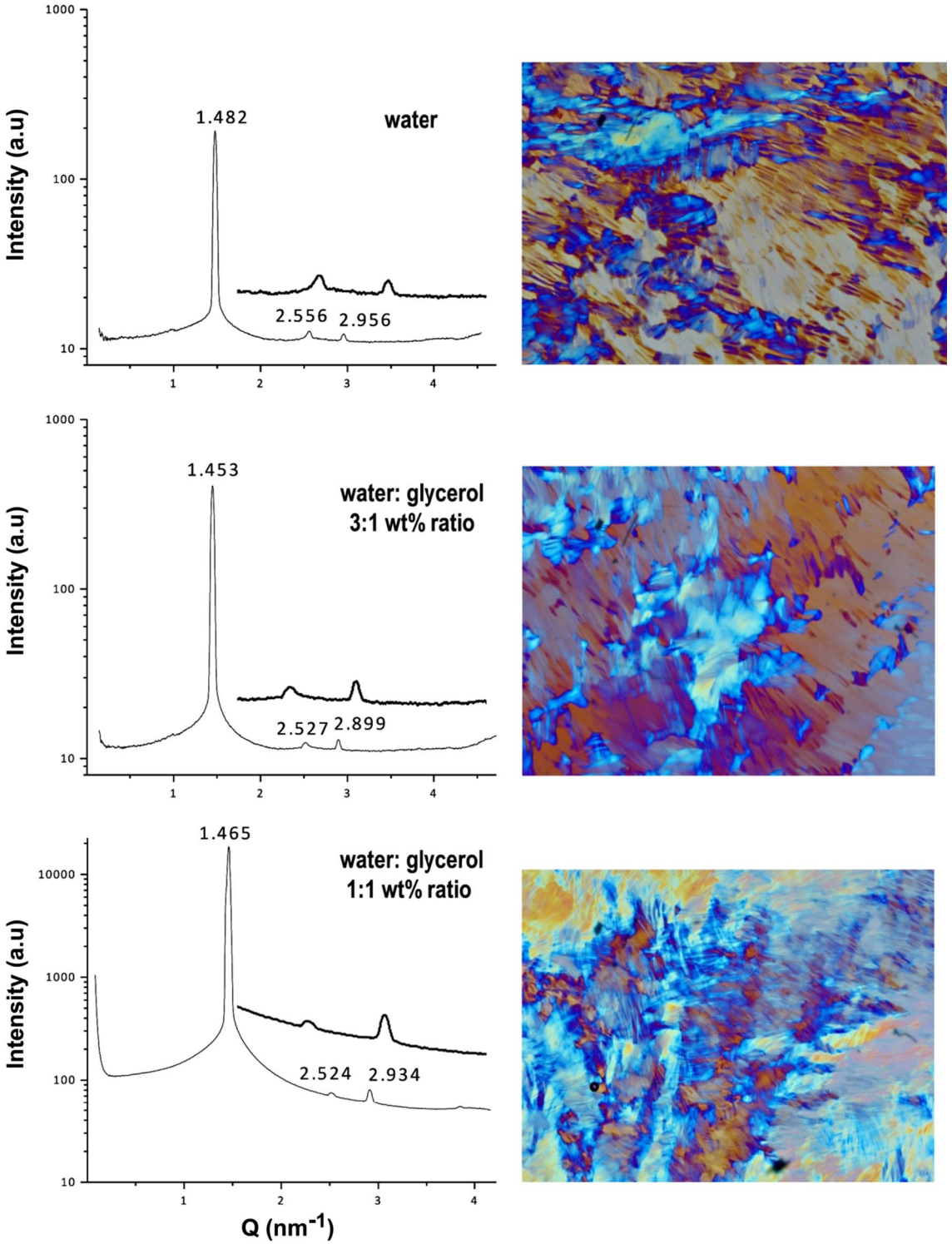

Fig. 4 SAXS measurement and polarized light microscope image obtained for systems I, II, and III, dilution line 8:2 (72 wt% GMO, 18 wt% decane, 10 wt% water; or water:glycerol (3:1 and, 1:1 wt% ratios)

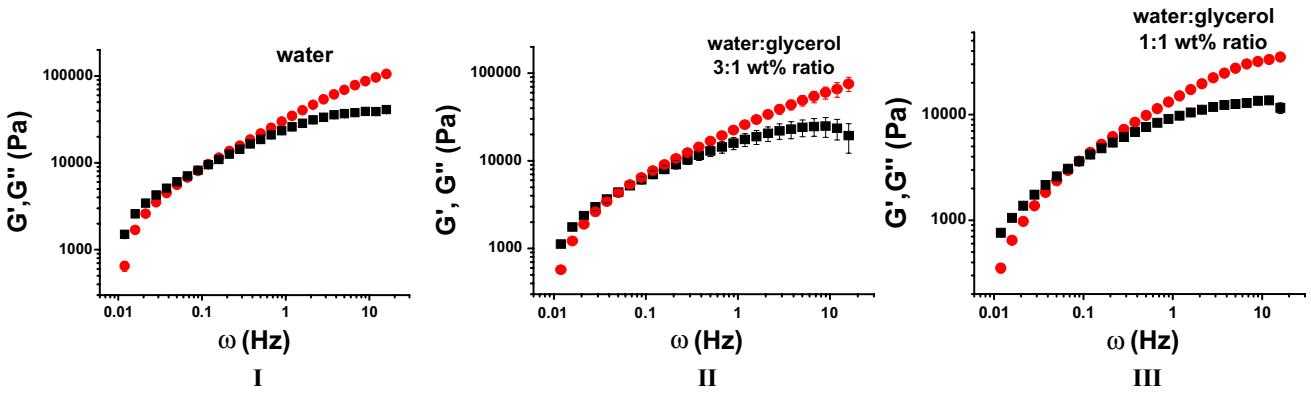

Fig. 5 Dynamic frequency sweep test for GMO/decane/water: glycerol system, dilution line 8:2 (72 wt% GMO, 18 wt% decane, 10 wt% water (I), and water:glycerol (3:1 (II) and 1:1 (III) wt ratios). *G′ red filled circles*, *G″ black squares* (color figure online)

CPLM and SAXS

Preliminary structure examination through a CPLM was implemented to reconfirm the absence of crystalline matter and the formation of LLC. The CPLM helped to distinguish between typical mesophases based on their characteristic textures. CPLM images (Fig. 4) displayed birefringent and typical colorful textures that were attributed to the H_{II} symmetry along the dilution line 8:2 throughout all the compositions and with any glycerol contents [72 wt% GMO, 18 wt% decane and 10 wt% of water; or water:glycerol (3:1 and 1:1 wt% ratio)]. In order to corroborate the presence of these structures in the mentioned system, SAXS analyses were performed.

SAXS profiles of dilution line 8:2 (72 wt% GMO, 18 wt% decane, 10 wt% water; or water:glycerol) in all the systems confirmed the existence of H_{II} mesophases with three characteristic diffraction peaks of the mesophase (Fig. 4). The increase in the lattice parameter is due to an increase in the GMO and water content. Glycerol has an additional swelling effect and an increase in the lattice parameter would be expected [28]. However, in a system poor in water (10 *vs* 20 %) and with less GMO, the swelling effect is expected to be less pronounced, and the effect of glycerol was less seen. This is the explanation for the fact that in the present systems, the lattice parameter increase was negligible: from 49 to 49.6 ± 0.5 Å.

Rheology Measurements

At low frequencies, all the systems were found to be more viscous than elastic ($G'' > G'$). Viscoelastic fluids are viscous at low frequencies with low elasticity. At higher angular frequency, G' and G'' reach a crossover point where G' dominates G''. From this point, the elastic properties of the system dominate ($G' > G''$), showing that the stored energy in the structure prevails over the energy dissipated by the viscous forces (Fig. 5). This behavior is called "transition to the flow region" [39]. This general trend of $G'(\omega)$ and $G''(\omega)$ is consistent with the behavior of hexagonal structures [30, 31, 40]. The hexagonal phase behaves as a viscoelastic fluid capable of flowing under shear at low frequencies but exhibiting an elastic behavior as soon as the frequency is increased, and with a response to shear characterized by a specific relaxation time [39].

All the systems also showed that at lower and higher frequencies the elasticity, plasticity, and viscosity decrease with the amount of glycerol (G', G'') (Figs. 5, 6). This clearly indicates that the structural modulation of the surfactant aggregates at the interface result in transformation to a more fluid structure due to an order–order transition [31, 41]. When water was replaced by 25 % glycerol no change was seen on the crossover between G' and G''. When 50 % was replaced by glycerol, the crossover shifted to higher frequencies, indicating a faster relaxation time, but H_{II} still remains its structure.

DSC

The thermotropic behavior of the system I (water) mixture during a heating scan from −40 to +80 °C (Fig. 7) revealed the presence of three endothermic events with three maxima at −33 °C, −5.33 °C, and 0 °C. The first endothermic event (peak) along the dilution line 8:2 corresponds to the melting of decane. The second and third peaks are of the complex mixture of GMO/glycerol and water, confirming that the water is in part bound and in part free (0 °C). There is also an endothermic event (small peak), at 18 °C that belongs to the formation of a lamellar phase that converts immediately upon further heating to H_{II} that is reflected as an exothermic peak at 22–23 °C.

In system II (water:glycerol wt% ratio 3:1) two endothermic peaks were recorded, the first of decane melting at −33 °C and the second of the combined mixture

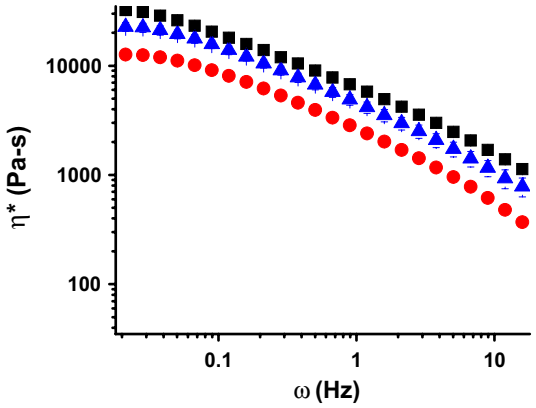

Fig. 6 Complex viscosity η^* of GMO/decane/water:glycerol system, dilution line 8:2 (72 wt% GMO, 18 wt% decane, 10 wt% water (I), and water:glycerol 3:1 (II) and, 1:1 (III) wt ratios. *Black squares* water, *blue triangles* water:glycerol 3:1 wt% ratio, *red filled circles* water:glycerol 1:1 wt% ratio (color figure online)

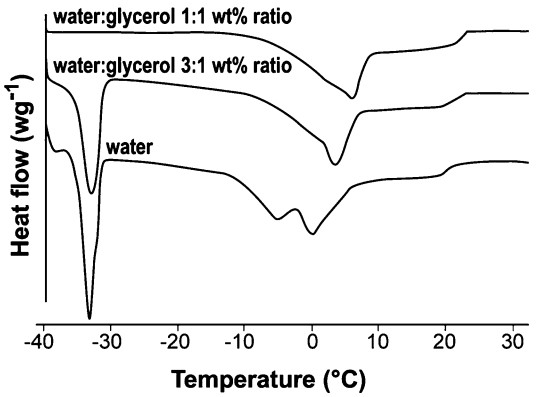

Fig. 7 DSC of GMO/decane/water: glycerol system, dilution line 8:2 (72 wt% GMO, 18 wt% decane, 10 wt% water (I), and water:glycerol 3:1(II) and 1:1 (III) wt ratios)

of GMO, water, and glycerol melting as a broad peak at 3 °C. Similarly to system I, a conversion from L_α to H_{II} phase took place at the same temperatures. In system III (water:glycerol wt% ratio 1:1) no melting peak of decane was found. This means that in this system decane is molecularly solubilized within the GMO/water/glycerol interfacial layer. An endothermic peak at 5 °C was recorded for the melting of this mixture, followed by the formation of L_α phase very fast and with minimum energy transition to H_{II} mesophases that took place at 22 °C. In system I, there seems to be a direct transformation from crystalline to $H_{II,}$ and in systems II and III, a solid–liquid transformation took place.

Glycerol influences the phase transformation of the system. When it is present, there is no bound water.

Conclusions

This study demonstrates that the water phase in the H_{II} mesophase can be partially replaced by glycerol, producing a disorder in the symmetry. Any further replacement will cause full destruction of the structure.

Only in limited regions of the phase diagram compositions (mostly regions rich in GMO) were H_{II} mesophases stable at room temperature. In most other regions the mesophases were an isotropic fluid composed of micro-droplets with undesired rheology properties.

Replacement of water by glycerol significantly increased the gel phase region in the phase diagram on the account of the H_{II} mesophase.

It is important to stress that exposing the systems to 37 °C (body temperature) caused a fast rearrangement of some of the structures, converting them to Newtonian low viscosity micro-droplets. These transitions have some advantages when preparing cosmetic body and face creams.

Recooling the system to 25 °C again changed the phase behavior and increased the viscosity of the system but left some of the compositions isotropic rather than liquid crystalline. The heating cooling process in certain selected compositions enabled reaching a new equilibration process of oleogels with fast settling of the gel phase with preferred rheology properties.

Glycerol also decreased the elasticity, plasticity, and viscosity of all three systems, emphasizing practical application in cosmetics.

Acknowledgments The authors acknowledge the Ph.D. Scholarship granted by the Center for Absorption in Science from the Ministry of Aliyah and Immigrant Absorption of Israel and, the Kaete Klausner Ph.D. Scholarship from the Hebrew University of Jerusalem granted by the Beethoven Foundation to Yael Cegla-Nemirovsky.

References

1. Terech P, Weiss RG (1997) Low molecular mass gelators of organic liquids and the properties of their gels. Chem Rev 97:3133–3159
2. Amar-Yuli I, Libster D, Aserin A, Garti N (2009) Solubilization of food bioactives within lyotropic liquid crystalline mesophases. Curr Opin Colloid Interface Sci 14:21–32
3. Efrat R, Abramov Z, Aserin A, Garti N (2010) Nonionic-anionic mixed surfactants cubic mesophases. Part I: structural chaotropic and kosmotropic effect. J Phys Chem B 114:10709–10716
4. Bot A, Floter E, Lammers JG, Pelan EG (2007) The texture and microstructure of spreads. In: McClements DJ (ed) Understanding and controlling the microstructure of complex foods. Woodhead Publ. Cambridge, pp 575–599
5. Marangoni AG (2004) Crystallization kinetics. In: Marangoni AG (ed) Fat crystal networks. Marcel Dekker, New York, pp 21–82
6. Pernetti M, van Malssen KF, Floter E, Bot A (2007) Structuring of edible oils by alternatives to crystalline fat. Curr Opin Colloid Interface Sci 12:221–231

7. Wright AJ, Marangoni AG (2006) Formation, structure, and rheological properties of ricinelaidic acid-vegetable oil organogels. J Am Oil Chem Soc 83:497–503
8. Daniel J, Rajasekharan R (2003) Organogelation of plant oils and hydrocarbons by long-chain saturated FA, fatty alcohols, wax esters, and dicarboxylic acids. J Am Oil Chem Soc 80:417–421
9. Rogers MA (2009) Novel structuring strategies for unsaturated fats - Meeting the zero-trans, zero-saturated fat challenge: a review. Food Res Int 42:747–753
10. Pernetti M, van Malssen K, Kalnin D, Floter E (2007) Structuring edible oil with lecithin and sorbitan tri-stearate. Food Hydrocolloids 21:855–861
11. Sagalowicz L, Leser ME, Watzke HJ, Michel M (2006) Monoglyceride self-assembly structures as delivery vehicles. Trends Food Sci Technol 17:204–214
12. Sein A, Verheij JA, Agterof WGM (2002) Rheological characterization, crystallization, and gelation behavior of monoglyceride gels. J Colloid Interface Sci 249:412–422
13. Marangoni AG, Idziak SHJ, Vega C, Batte H, Ollivon M, Jantzi PS, Rush JWE (2007) Encapsulation-structuring of edible oil attenuates acute elevation of blood lipids and insulin in humans. Soft Matter 3:183–187
14. Heertje I, Roijers EC, Hendrickx H (1998) Liquid crystalline phases in the structuring of food products. Food Sci Technol Lebensm Wiss Technol 31:387–396
15. Ojijo NKO, Kesselman E, Shuster V, Eichler S, Eger S, Neeman I, Shimoni E (2004) Changes in microstructural, thermal, and rheological properties of olive oil/monoglyceride networks during storage. Food Res Int 37:385–393
16. Kesselman E, Shimoni E (2007) Imaging of oil/monoglyceride networks by polarizing near-field scanning optical microscopy. Food Biophys 2:117–123
17. Kaneko F (2001) Polymorphism and phase transitions of fatty acids and acylglycerols. In: Garti N, Sato K (2001) Crystallization processes in fats and lipids systems. Marcel Dekker, New York, pp 53–60
18. Chen CH, Terentjev EM (2009) Aging and metastability of monoglycerides in hydrophobic solutions. Langmuir 25:6717–6724
19. Chen CH, Terentjev EM (2010) Effects of water on aggregation and stability of monoglycerides in hydrophobic solutions. Langmuir 26:3095–3105
20. Vauthey S, Visani P, Frossard P, Garti N, Leser ME, Watzke HJ (2000) Release of volatiles from cubic phases: monitoring by gas sensors. J Dispersion Sci Technol 21:263–278
21. Caboi F, Nylander T, Razumas V, Talaikyte Z, Monduzzi M, Larsson K (1997) Structural effects, mobility, and redox behavior of vitamin K-1 hosted in the monoolein/water liquid crystalline phases. Langmuir 13:5476–5483
22. Suzuki T, Nakamura M, Sumida H, Shigeta A (1992) Liquid crystal make-up remover—conditions of formation and its cleansing mechanisms. J Soc Cosmet Chem 43:21–36
23. Engstrom S, Lindahl L, Wallin R, Engblom J (1992) A study of polar lipid drug carrier systems undergoing a thermoreversible lamellar-to-cubic phase transition. Int J Pharm 86:137–145
24. Boyd BJ, Khoo SM, Whittaker DV, Davey G, Porter CJH (2007) A lipid-based liquid crystalline matrix that provides sustained release and enhanced oral bioavailability for a model poorly water soluble drug in rats. Int J Pharm 340:52–60
25. Hung LC, Ismail R, Basri M, Nang HLL, Tejo BA, Abu Hassan H, May CY (2010) Testing of glyceryl monoesters for their antimicrobial susceptibility and their influence in emulsions. J Oil Palm Res 22:846–855
26. Co ED, Marangoni AG (2012) Organogels: an alternative edible oil-structuring method. J Am Oil Chem Soc 89:749–780
27. Amar-Yuli I, Garti N (2005) Transitions induced by solubilized fat into reverse hexagonal mesophases. Colloids Surf B 43:72–82
28. Amar-Yuli I, Azulay D, Mishraki T, Aserin A, Garti N (2011) The role of glycerol and phosphatidylcholine in solubilizing and enhancing insulin stability in reverse hexagonal mesophases. J Colloid Interface Sci 364:379–387
29. Drummond CJ, Fong C (1999) Surfactant self-assembly objects as novel drug delivery vehicles. Curr Opin Colloid Interface Sci 4:449–456
30. Mishraki T, Libster D, Aserin A, Garti N (2010) Lysozyme entrapped within reverse hexagonal mesophases: physical properties and structural behavior. Colloids Surf B 75:47–56
31. Libster D, Aserin A, Wachtel E, Shoham G, Garti N (2007) An H-II liquid crystal-based delivery system for cyclosporin A: physical characterization. J Colloid Interface Sci 308:514–524
32. Gekko K, Timasheff SN (1981) Mechanism of protein stabilization by glycerol—preferential hydration in glycerol—water-mixtures. Biochemistry 20:4667–4676
33. Kumar A, Kunieda H, Vazquez C, Lopez-Quintela MA (2001) Studies of domain size of hexagonal liquid crystals in $C_{12}EO_8$/water/alcohol systems. Langmuir 17:7245–7250
34. Iwanaga T, Suzuki M, Kunieda H (1998) Effect of added salts or polyols on the liquid crystalline structures of polyoxyethylene-type nonionic surfactants. Langmuir 14:5775–5781
35. Alam MM, Shrestha LK, Aramaki K (2009) Glycerol effects on the formation and rheology of cubic phase and related gel emulsion. J Colloid Interface Sci 329:366–371
36. Alam MM, Aramaki K (2009) Glycerol effects on the formation and rheology of hexagonal phase and related gel emulsion. J Colloid Interface Sci 336:820–826
37. Krog N, Larsson K (1968) Phase behavior and rheological properties of aqueous systems of industrial distilled monoglycerides. Chem Phys Lipids 2:129–143
38. Gurfinkel J, Aserin A, Garti N (2011) Interactions of surfactants in nonionic/anionic reverse hexagonal mesophases and solubilization of alpha-chymotrypsinogen A. Colloids Surf A 392:322–328
39. Mezzenga R, Meyer C, Servais C, Romoscanu AI, Sagalowicz L, Hayward RC (2005) Shear rheology of lyotropic liquid crystals: a case study. Langmuir 21:3322–3333
40. Libster D, Aserin A, Yariv D, Shoham G, Garti N (2009) Concentration- and temperature-induced effects of incorporated desmopressin on the properties of reverse hexagonal mesophase. J Phys Chem B 113:6336–6346
41. Sagalowicz L, Mezzenga R, Leser ME (2006) Investigating reversed liquid crystalline mesophases. Curr Opin Colloid Interface Sci 11:224–229